Carcinogenesis, 2019, Vol. 40, No. 12, 1469–1479

doi:10.1093/carcin/bgz071
Advance Access Publication April 17, 2019
Original Article

ORIGINAL ARTICLE

circRAD18 sponges miR-208a/3164 to promote triple-negative breast cancer progression through regulating IGF1 and FGF2 expression

Yutian Zou†, Shaoquan Zheng†, Weikai Xiao†, Xinhua Xie, Anli Yang, Guanfeng Gao, Zhenchong Xiong, Zhicheng Xue, Hailin Tang* and Xiaoming Xie*

Department of Breast Oncology, Sun Yat-sen University Cancer Center, State Key Laboratory of Oncology in South China, Collaborative Innovation Center for Cancer Medicine, 651 East Dongfeng Road, Guangzhou 510060, People's Republic of China.

*To whom correspondence should be addressed. E-mail: xiexm@sysucc.org.cn
Correspondence may also be addressed to Hailin Tang; E-mail: tanghl@sysucc.org.cn
†These authors contributed equally to this work.

Abstract

As a new rising star of non-coding RNA, circular RNAs (circRNAs) emerged as vital regulators with biological functions in diverse of cancers. However, the function and precise mechanism of the vast majority of circRNAs in triple-negative breast cancer (TNBC) occurrence and progression have not been clearly elucidated. In the current study, we identified and further investigated hsa_circ_0002453 (circRAD18) by analyzing our previous microarray profiling. Expression of circRAD18 was found significantly upregulated in TNBC compared with normal mammary tissues and cell lines. circRAD18 was positively correlated with T stage, clinical stage and pathological grade and was an independent risk factor for TNBC patients. We performed proliferation, colony formation, cell migration, apoptosis and mouse xenograft assays to verify the functions of circRAD18. Knockdown of circRAD18 significantly suppressed cell proliferation and migration, promoted cell apoptosis and inhibited tumor growth in functional and xenograft experiments. Through luciferase reporter assays, we confirmed that circRAD18 acts as a sponge of miR-208a and miR-3164 and promotes TNBC progression through upregulating *IGF1* and *FGF2* expression. Altogether, our research revealed the pivotal role of circRAD18-miR-208a/3164-*IGF1*/*FGF2* axis in TNBC tumorigenesis and metastasis though the mechanism of competing endogenous RNAs. Thus, circRAD18 may serve as a novel prognostic biomarker and potential target for TNBC treatment in the future.

Introduction

Breast cancer is known as the most pervasive cancer and the second leading cause of cancer-related death among women according to the global estimated cancer statistics (1). It is predicted that there will be 268 600 new cases and 42 260 deaths of female breast cancer in the USA in 2019 (2). Breast cancer is acknowledged as a heterogeneous disease with four major different molecular subtypes (3). Among them, triple-negative breast cancer (TNBC) accounts for approximately 15–20% of all breast cancer cases, which remains a challenging obstacle for oncological therapy for its poor prognosis (4–6). Therefore, identifying more efficient therapeutic molecular targets and developing novel prognostic biomarkers for TNBC is an imperative need.

Circular RNAs (circRNAs) attracted tremendous attention and became one of the research hotspots for their impact on the occurrence and progression of cancer in recent years (7). Once regarded as byproducts of erroneous splicing, circRNAs are one type of non-coding RNAs (ncRNAs), which widely exist and express in mammals (8). Highly conversed and stable, circRNAs form single-stranded and covalently

Received: January 28, 2019; **Revised:** March 13, 2019; **Accepted:** April 15, 2019

Abbreviations

3'-UTR	3'-untranslated region
ANOVA	analysis of variance
circRNA	circular RNA
ceRNA	competing endogenous RNAs
EdU	5-Ethynyl-20-deoxyuridine
FGF2	fibroblast growth factor 2
HER2	human epidermal growth factor receptor 2
IGF1	insulin-like growth factor 1
lncRNA	long non-coding RNA
miRNA	microRNA
MRE	miRNA response element
mRNA	messenger RNA
NC	negative control
ncRNA	non-coding RNA
PI	propidium iodide
siRNA	small interfering RNA
TNBC	triple-negative breast cancer

closed loops with no 5'-cup and 3'-poly A tail (9). Both *cis*-elements and *trans*-acting factors participate in the formation of circRNA by the back splicing of exons or introns (10,11). With the progress and development made in high-throughput RNA-Seq technology nowadays, circRNAs are widely studied and found to play a pivotal role in a diversity of cancers as microRNA (miRNA) sponges, RNA-binding protein regulators, protein-coding templates and so on (12). According to the competing endogenous RNA (ceRNA) theory presented by Pandolfi *et al*., messenger RNAs (mRNAs), pseudogenes and long non-coding RNAs (lncRNAs) can regulate and communicate mutually by binding to the miRNA response elements (MREs) (13). CircRNAs were discovered to be ceRNAs as well soon after (14). For instance, one of the most well-known circRNAs, ciRS-7, regulates cell signaling pathway and cancer-related genes by sponging miR-7 in multiple cancers (15–18). Another famous molecule, circHIPK3, acts as ceRNA with cancer suppressor gene mRNA and inhibits cell proliferation by regulating miR-124 in numerous cancers (19). In our previous study, circEPSTI1 was demonstrated to be a cancer-promoting circRNA by binding miR-4753/6809 and regulating *BCL11A* expression in TNBC (20). However, the potential biological functions and underlying molecular mechanisms of most circRNAs in development and progression in TNBC have not been clearly elucidated.

In the current study, we identified circRAD18 as one of the critical circRNAs that frequently upregulated in TNBC tissues by analyzing our previous microarray profiling. We next validated that circRAD18 was positively correlated with T stage, clinical stage and pathological grade. Univariate and multivariate Cox regression analysis revealed that circRAD18 level was an independent risk factor for TNBC patients. Further functional and mechanistic experiments revealed that circRAD18 promoted cell proliferation, migration and suppressed cell apoptosis by serving as a sponge for the miR-208a/3164 to relieve silence for target gene *IGF1* and *FGF2*. Both *in vitro* and *in vivo* assays verified the influence of circRAD18-miR-208a/3164-*IGF1/FGF2* axis on cancer proliferation and progression in TNBC. Generally, our research revealed that circRAD18 might serve as an oncogenic gene in TNBC tumorigenesis and metastasis, which could be a novel prognostic biomarker and potential target for TNBC treatment.

Materials and methods

Clinical data and patient samples

Fresh tumor tissues and its adjacent non-cancerous mammal tissues were collected from TNBC patients who received therapy at Sun Yat-Sen University Cancer Centre (SYSUCC, Guangzhou, Guangdong, China). All resected samples were immediately stored in RNAlater (Ambion, TX). Clinical data of the patients with TNBC were collected and all the patients were followed up regularly. This study was approved by the Ethics Committee of SYSUCC Health Authority and conducted in accordance with Declaration of Helsinki. Written informed consent was obtained from all patients before participation in this study.

Cell culture

Ten human breast cancer immortalized cell lines (MDA-MB-231, MDA-MB-468, BT549, HCC38, HCC1806, MCF-7, T47D, MDA-MB-453, BT474 and Skbr-3), normal mammary epithelial cell lines (MCF-10A) and human embryonic kidney (HEK-293T) cells were all purchased from American Type Culture Collection (Manassas, VA) and were passaged for less than 6 months. Cultured according to the instruction of the supplier, all above cell lines were tested for mycoplasma infection and authenticated by DNA profiling occasionally.

RNA preparation and qRT-PCR

TRIzol reagent (Life Technologies) was used to isolate total RNA. RNA isolation of nuclear and cytoplasmic portions was conducted utilizing NE-PER Nuclear and Cytoplasmic Extraction Reagents (Thermo Scientific). Complementary DNAs (cDNAs) were reversely transcribed using the Prime Script RT reagent kit (Takara, Japan). quantitative real-time polymerase chain reaction (qRT-PCR) was conducted with SYBR Premix Ex Taq (Takara, Japan). Primer information is listed in Supplementary Table S1.

RNase R treatment

RNase R (Epicentre Technologies) was performed in order to digest linear RNAs. RNAs extracted from MDA-MB-231 cells were equally divided into two parts: one was for RNase R treatment and another was for control with buffer only. 2 μg of total RNA was incubated for 20 min at 37°C with RNase R (3U/μg) in treatment group. We used β-actin in control group as internal control.

Actinomycin D assay

Into six-well plates, 1×10^5 cells were seeded and subjected to 2 mg Actinomycin D (Sigma) for 8, 16 and 24 h. Subsequently, the treated cells were collected at the specific time periods for qRT-PCR analysis of circRAD18 or RAD18 mRNA.

Oligonucleotide transfection

Transfection was performed utilizing Lipofectamine 2000 (Invitrogen). The small interfering RNAs (siRNAs) were provided by RiboBio (Guangzhou, China). The miRNA inhibitors and mimics were synthesized by GeneCopoeia (Rockville, MD).

CCK-8 assay

Cell proliferation was evaluated by cell counting kit-8 (CCK-8) assay kit (Dojindo Corp, Japan). In all, 1×10^3 cells were seeded in each well of a 96-well plate. 10 μl of CCK-8 solution was added to each well on the indicated day. Afterwards, the cells were incubated with CCK-8 solution for 2 h at 37°C, and the absorbance was assessed at 450 nm wavelength through a microtiter plate reader.

Colony formation assay

At a density of 1×10^3 cells per well, the resuspended cells were replanted in six-well plates and maintained for 10 days. Cell were fixed by 100% methanol and dyed by 0.5% crystal violet for 30 min. Colonies were subsequently photographed and counted.

Apoptosis assay and 5-Ethynyl-2'-deoxyuridine assay

Cell apoptosis were detected by Annexin V/propidium iodide (PI) staining and flow cytometry using the Andy Fluor 488 Annexin V/PI Kit (GeneCopoeia). Cell proliferative activity was assessed using the IClick™ 5-Ethynyl-20-deoxyuridine (EdU) Andy Fluor™ 488 Flow Cytometry Assay Kit (GeneCopoeia). 10 μM EdU was added to MDA-MB-231, MDA-MB-468 and BT549 for 4 h before flow cytometry analysis.

Wound-healing assay and transwell assay

For wound-healing assay, TNBC cells were planted in six-well plates and transfected with siRNA or si-negative control (NC). A linear wound was scratched with a sterile 200 μl pipette tip and were imaged by inverted microscope at 0 h and 24 h time period, next analyzed utilizing Image J software. Transwell assays were conducted with migration upper chambers (BD Biosciences). To the upper chambers, 2×10^4 TNBC cells were suspended and added, whereas medium (with 20% fetal bovine serum) was added into the lower chambers. After 24 h, we removed the upper chambers cells and fixed the remaining cells in methanol, stained by crystal violet and then counted after photographing.

Dual-luciferase reporter assay

HEK-293T cells were planted into 96-well plates with 5×10^3 cells per well. After transiently transfected with constructed plasmids and miRNA inhibitors or mimics for 48 h, luciferase activity was evaluated by the dual-luciferase reporter assay system (Promega) according to the manufacturer's instructions. We detected renilla luciferase activity as internal control. Independent experiments were conducted in triplicate.

Plasmid constructs

To construct a circRAD18 plasmid, full-length human circRAD18 cDNA was amplified and cloned into pCDNA3.0 vector in the downstream of a Cytomegalovirus promoter-driven luciferase. The mutant circRAD18 and *IGF1*/*FGF2* 3'-untranslated region (UTR) were generated by mutating the conserved miRNA binding sites using Gene Mutation Kit (Takara, Japan). Sequencing was used to confirm all the plasmid constructs before luciferase reporter assay.

Western blot analysis

Total cell protein was extracted applied by RIPA lysis buffer with proteinase inhibitor (Thermo). Equal amounts of protein in the lysates was separated by 12% sodium dodecyl sulfate–polyacrylamide gel electrophoresis and transferred onto polyvinylidene difluoride membranes. After being blocked by 5% skim milk powder for 1 h, the transferred membranes were then incubated overnight at 4°C with IGF1 antibody (Abcam, 1:1000), FGF2 antibody (Abcam, 1:1000), RAD18 antibody (Abcam, 1:1000) and β-actin antibody (CST, 1:5000). Then, secondary antibodies were used at a dilution of 1:5000 to incubate membranes at room temperature for 1 h. Enhanced chemiluminescence detection reagents (ECL New England Biolabs) were used to visualize the specific protein.

In vivo tumor growth assays

All animal care and procedures were performed in accordance with the guidelines of the Institutes and the approval of Institute Research Ethics Committee of SYSUCC. In order to investigate the effect of circRAD18 on tumorigenesis, two TNBC cell lines MDA-MB-231 and BT549 (1×10^7 cells per mouse) were subcutaneously injected into the dorsal flanks of 4-week-old female BALB/c nude mice (three in each group) and treated with intertumoral injection (40 μl si-circRAD18 or si-NC) in phosphate-buffered saline every 4 days. Tumor diameters were measured and recorded every 4 days. We calculated tumor volumes (mm^3) with the following formula: volume = (width^2 × length)/2. On day 28, mice were killed by euthanasia and subcutaneous xenografts were collected.

Analysis of public databases

To evaluate the prognostic value of hsa-miR-208a and hsa-miR-3164 in TNBC patients, we analyzed the Kaplan–Meier plotter database on the website http://kmplot.com/analysis/. The auto-selected values were set as the cutoff values to plot the survival curves and conducted the log-rank method.

Statistical analysis

All data were analyzed using SPSS 25.0 software (SPSS, Chicago, IL). All quantitative data were presented as the mean ± standard deviation. Two-tailed Student's *t*-test or one-way analysis of variance (ANOVA) were implemented to determine statistically significant differences between two or multiple groups, respectively. The correlation of circRAD18 expression level with clinicopathological features of TNBC patients was analyzed by χ^2 test. The Kaplan–Meier analysis was applied to calculate the overall survival curves and the log-rank test was implemented to compare differences between two groups. $P < 0.05$ was considered statistically significant.

Results

Characterization of circRAD18 and its association with clinicopathologic feature in TNBC patients

Analyzing our previous microarray profiling, we identified that the expression of hsa_circ_0002453 in TNBC is 2.87 times higher than that in adjacent normal tissues (20). According to the University of California Santa Cruz Genome Browser and circBase database, hsa_circ_0002453 is derived from exons 3, 4, 5, 6 and 7 of *RAD18* (RAD18, E3 ubiquitin protein ligase) located on chromosome 3p25 (chr3: 8977554-8990254), with exon 3 and 7 back spliced (756 bp). We named hsa_circ_0002453 as circRAD18, which could be amplified by divergent primers and further confirmed by Sanger DNA sequencing and gel electrophoresis (Figure 1A and Supplementary Figure S1A). We validated circRAD18 expression level in 31 pairs of TNBC tissues and adjacent mammary tissues using qRT-PCR, among which circRAD18 was overexpressed in 27 pairs (87%) (Supplementary Figure 1B and C). In addition, the expression of circRAD18 was correlated with the T stage, clinical stage and pathological grade in 126 TNBC tissues (Figure 1D and E and Supplementary Figure S1B). Consistently, circRAD18 expression was positively correlated with the T stage, tumor size and clinical stage (P = 0.001, 0.002 and 0.010, respectively) in TNBC patients (Supplementary Table S2). Further univariate and multivariate Cox regression analysis indicated that high circRAD18 expression was shown as an independent risk factor for TNBC patients (Supplementary Table S3). Besides, Kaplan–Meier survival analysis displayed a poorer overall survival (OS) of TNBC patients with high circRAD18 level (P = 0.014; Figure 1F). Receiver operating characteristic curve analysis revealed that circRAD18 could be used as a diagnostic index differentiating TNBC from normal mammary tissues (Supplementary Figure S1C). In agreement with above results from TNBC patients, circRAD18 levels are higher in eight breast cancer cell lines, particularly in TNBC cell lines (MDA-MB-231, MDA-MB-468, BT549, HCC1806 and HCC38; Figure 1G). To further verify its circular characteristics, circRAD18 was resistant to 3' to 5' exoribonuclease RNase R in contrast to linear RAD18 mRNA (Figure 1H). Actinomycin D assays exhibited that circRAD18 showed an exceeded half life (more than 24 h) with higher stability than the RAD18 linear RNA transcript (less than 8 h) in MDA-MB-231 cells (Figure 1I). Moreover, circRAD18 predominantly resided in the cytoplasm, detected by qRT-PCR analysis of nuclear and cytoplasmic RNAs separated from MDA-MB-231 cells (Figure 1J).

circRAD18 promotes proliferation, metastasis and inhibits apoptosis of TNBC cell lines *in vitro*

To gain insights into the biological roles of circRAD18, we designed siRNA covering the back-splicing region for silencing,

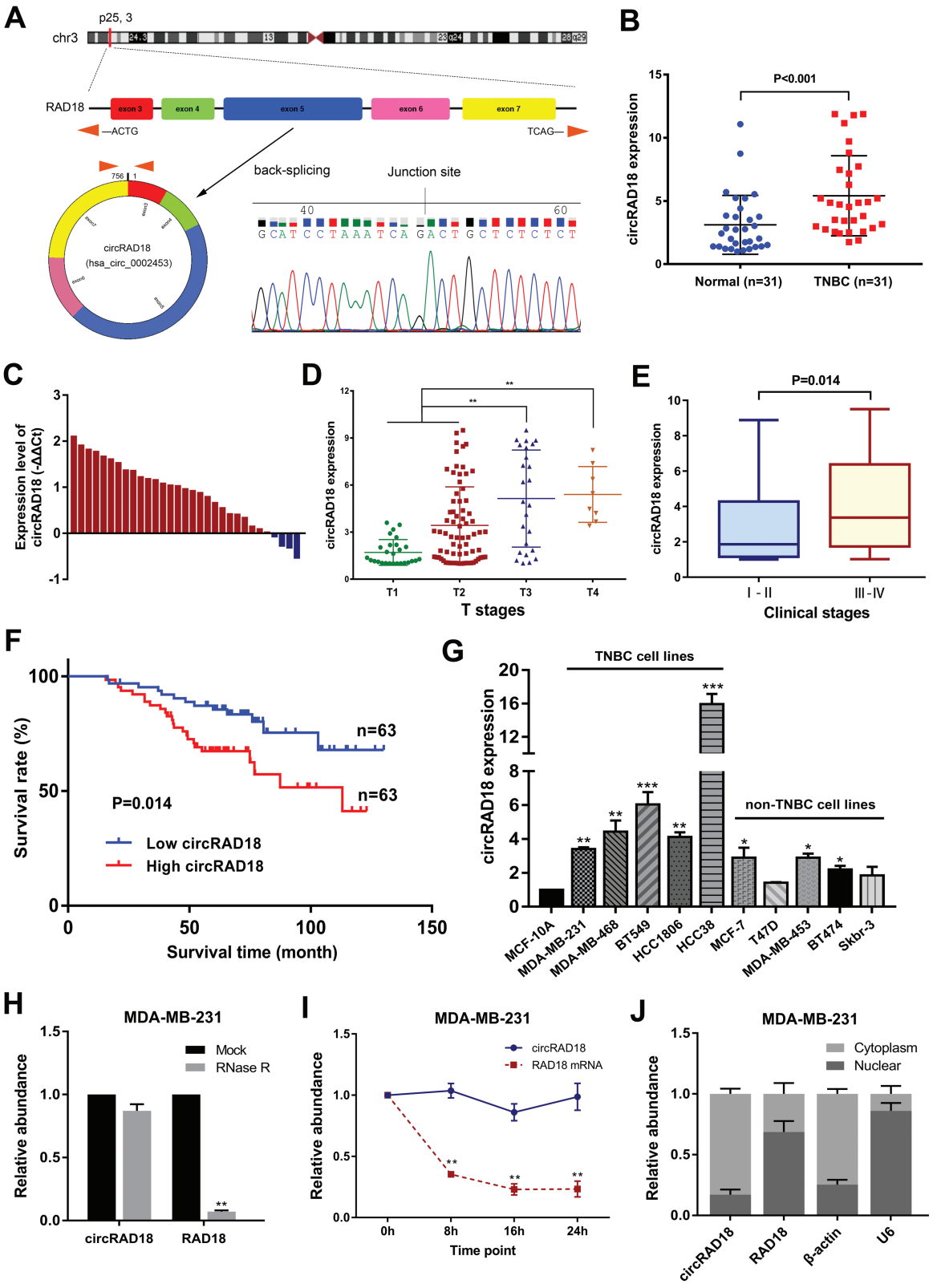

Figure 1. Characterization of circRAD18 and its association with clinicopathologic feature in TNBC patients. **(A)** The genomic loci of RAD18 gene and formation of circRAD18. The existence of circRAD18 was detected by Sanger DNA sequencing. **(B)** qRT-PCR analysis of circRAD18 level normalized by β-action in 31 pairs of TNBC and adjacent mammary tissues. **(C)** qRT-PCR analysis of circRAD18 levels calculated by -ΔΔCt (ΔCt(TNBC)-ΔCt (normal)). **(D and E)** Correlation between circRAD18 expression and T stage ($P < 0.01$, one-way ANOVA) and clinical stage in 126 cases of TNBC tumor tissues detected by qRT-PCR analysis. **(F)** Kaplan–Meier analysis of the overall survival of 126 TNBC patients with circRAD18 high (red) or low (blue) expression levels ($P = 0.014$). **(G)** The relative expression level of circRAD18 was determined in diverse mammary cell lines (including 1 normal and 10 breast cancer cell lines). **(H)** circRAD18 and RAD18 mRNA abundance in MDA-MB-231 cells after being treated with RNase R analyzed by qRT-PCR. **(I)** circRAD18 and RAD18 mRNA abundance after being treated with Actinomycin D in MDA-MB-231 cells analyzed by qRT-PCR. **(J)** U6 (nuclear control transcript), β-action mRNA (cytoplasmic control transcript), circRAD18 and RAD18 mRNA in nuclear and cytoplasmic fractions analyzed by qRT-PCR. *$P < 0.05$; **$P < 0.01$.

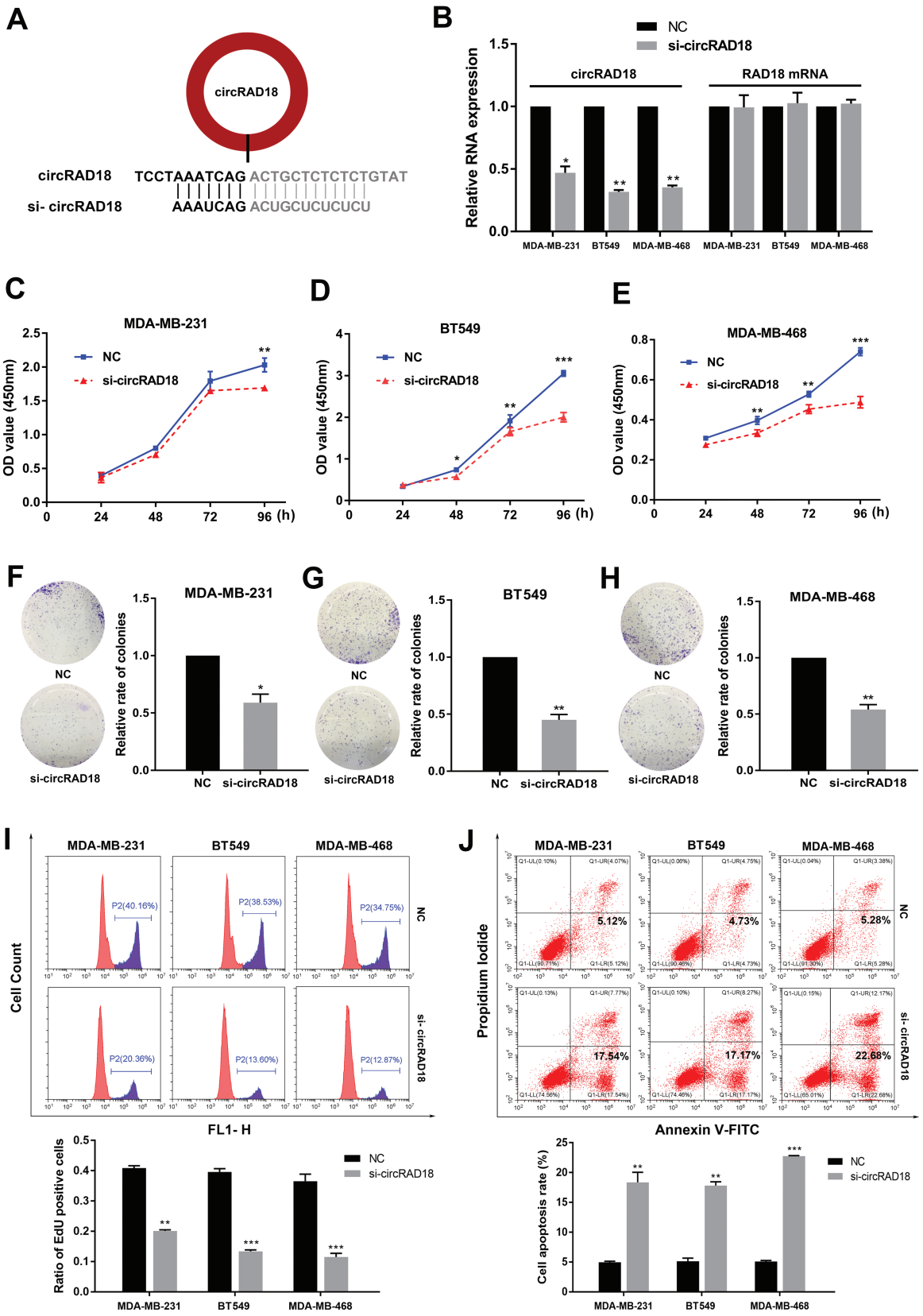

Figure 2. circRAD18 promotes proliferation and inhibits apoptosis of TNBC cell lines. **(A)** Schematic illustration showed siRNA targets the back-splice covalent junction of circRAD18. **(B)** Expression of circRAD18 and *RAD18* mRNA was assessed by qRT-PCR analysis after treatment with si-circRAD18. **(C–E)** CircRAD18 promotes the proliferation of MDA-MB-231, BT549 and MDA-MB-468 cells shown via the CCK-8 assays. **(F–H)** circRAD18 promotes the colony-forming ability of MDA-MB-231, BT549 and MDA-MB-468 cells shown by the colony formation assays. **(I)** EdU assays evaluated DNA synthesis efficiency of MDA-MB-231, BT549 and MDA-MB-468 cells. **(J)** Apoptosis rate examined by Annexin V-FITC/PI staining and fluorescence-activated cell sorting quantification in MDA-MB-231, BT549 and MDA-MB-468 cells. $^{*}P < 0.05$; $^{**}P < 0.01$; $^{***}P < 0.001$.

which did not affect RAD18 linear mRNA and RAD18 protein expression in MDA-MB-231, BT549 and MDA-MB-468 cell lines (Figure 2A and B and Supplementary Figure S2). Subsequently, we conducted CCK-8 and colony formation assays to assess the influence of circRAD18 on TNBC cell growth and proliferation. Downregulation of circRAD18 significantly inhibited cell growth and colony-forming ability of three TNBC cell lines in CCK-8 and colony formation assays, respectively (Figure 2C–H). Additionally, EdU assays were also conducted to determine proliferative ability, which was suppressed by silencing of circRAD18 (Figure 2I). In order to evaluate the impact of circRAD18 on cell apoptosis, three TNBC cell lines were transfected with siRNA for 48 h before Annexin V-fluorescein isothiocyanate (FITC)/PI staining. Results of flow cytometry-manifested downregulation of circRAD18 observably promoted the apoptosis of TNBC cell lines *in vitro* (Figure 2J). To examine the effects of circRAD18 on metastatic ability of TNBC cell, wound-healing and transwell assays were also carried out. Our results showed that knockdown of circRAD18 could significantly inhibit migration capability of three TNBC cell lines, demonstrated by wound-healing assays (Figure 3A–F) and transwell assays (Figure 3G–L).

circRAD18 serves as a sponge for miR-208a and miR-3164 in TNBC

Considering circRAD18 is preferentially localized and stable in the cytoplasm, we explored whether circRAD18 can bind to certain miRNAs as a miRNA sponge and promote tumorigenesis of TNBC. According to MREs analysis, four miRNAs were identified, whereas 64 miRNAs were found by searching circBank database (http://www.circbank.cn/). Three miRNAs (miR-208a, miR-3120-5p and miR-3164) were predicted by both algorithms (Figure 4A). We further analyzed the miRNA microarray data derived from TCGA and discovered that low expression of miR-208a and miR-3164 were both associated to worse OS with very similar Kaplan–Meier plots in TNBC patients (http://kmplot.com/analysis/; Figure 4B). circRAD18 sequence contains two potential binding sites of each miRNA and the relative sponging position on the circle was showed (Figure 4C and D). Thus, luciferase reporter assays were performed to confirm the interactions between miR-208a/miR-3164 and circRAD18. We first co-transfected a luc-circRAD18-wt or a luc-circRAD18-mut report vector, with each miRNA mimics or NC in HEK-293T cells, respectively. Overexpression of miR-208a or miR-3164 reduced the relative luciferase activity of a wild-type reporter by almost 50%, whereas it had no impact on the mutant one (Figure 4E). Consistently, relative luciferase intensity elevated when HEK-293T cells were co-transfected with wild-type luciferase report vectors and miR-208a/miR-3164 inhibitors (Figure 4F). This result demonstrated that circRAD18 acts as an endogenous sponge by binding miR-208a and miR-3164. In addition, clone formation assay revealed that the inhibition of miR-208a or (and) miR-3164 remarkably increased the colony-forming ability of MDA-MB-231 cells, and this effect could be blocked by circRAD18 knockdown (Figure 4G).

circRAD18 promotes TNBC cell growth and proliferation via circRAD18-miR-208a/3164-IGF1/FGF2 axis

To explore the potential co-target oncogenes of miR-208a and miR-3164, three algorithms (TargetScan (21), TargetMiner (22) and miRDB (23)) were used to predict putative genes (Figure 5A). Among the candidate co-targeted genes, *IGF1* was predicted by all three algorithms, whereas *FGF2* was identified by TargetScan and TargetMiner (Figure 5B). *IGF1* and *FGF2* plays a crucial part in the progression of various malignancies, including breast cancer, by promoting cancer cell proliferation, invasion and tumor angiogenesis (24–31). To confirm this speculation, the 3'-UTR and its mutated sequence of *IGF1* and *FGF2* were separately constructed downstream of luciferase gene into the pGL3 reporter plasmid. Luciferase reporter vector was transfected into HEK-293T cells alone or together with miR-208a and miR-3164 or both. Relative luciferase density was significantly decreased after co-transfection of miRNA mimics with wt-3'UTR of *IGF1* or *FGF2* plasmid compared with the mutant one (Figure 5C and D). In contrast, relative luciferase activity was significantly increased after co-transfection of *IGF1* or *FGF2* wt-3'UTR vector with miR-208a inhibitors and miR-3164 inhibitors, respectively, or both (Figure 5E and F). These results confirmed that miR-208a and miR-3164 could bind to the 3'-UTR of *IGF1* or *FGF2*. We next performed experiments to verify whether circRAD18 functions via circRAD18-miR-208a/3164-*IGF1*/*FGF2* axis in TNBC cells. We found knockdown of circRAD18 reduced the luciferase activity of *IGF1* or *FGF2* wt-3'UTR reporter (Figure 5G). Moreover, qRT-PCR and western blot analysis showed that miR-208a/3164 mimics or si-circRAD18 could not only change the mRNA level of both two target genes but also reduce the expression of their protein (Figure 5H–J and Supplementary Figure S3A–D).

circRAD18 promotes TNBC tumorigenesis *in vivo*

Mouse xenograft models were constructed to explore the biological influence of circRAD18 on tumor growth *in vivo*. MDA-MB-231 and BT549 cells were subcutaneously injected into nude mice before continuous intertumoral injection of si-circRAD18 or NC siRNAs. A significant reduction in tumor growth (Figure 6A and B) and tumor weight (Figure 6C and D) was found by knockdown of circRAD18 compared with NC siRNAs. These results indicated that circRAD18 could promote TNBC tumorigenesis via circRAD18-miR-208a/3164-*IGF1*/*FGF2* axis *in vivo*.

Discussion

With the innovation and progress made in bioinformatics and high-throughput RNA-Seq technologies, an increasing number of circRNAs have been convinced as large group of endogenous ncRNAs in recent years (32). CircRNAs are naturally generated, covalently closed and single-stranded transcripts, which are much stably existed in cytoplasm compared with linear RNAs (9). The significant role of circRNAs in carcinogenesis appealed to more and more researchers and have become a hot topic in cancer research in a short term. On the one hand, some upregulated circRNAs like circPRKCI (33), ciRS-7 (15–18), circCTIC1 (34), circEPSTI1 (20) and circGFRA1 (35) function as oncogenes in the tumorigenesis and progression of various cancers. On the other hand, a substantial number of circRNAs like circHIPK3 (19), circLARP4 (36) and circZKSCAN1 (37) inhibit tumor growth by regulating multiple signaling pathways. Moreover, as a highly stable and free RNA, circRNA can also be detected in exosomes according to several studies in recent years. For example, researchers have convinced the presence of circPRMT5 in serum and urine exosomes of patients with urothelial carcinoma of the bladder (38). circPDE8A was discovered in pancreatic ductal adenocarcinoma excreted exosomes which could enter into blood circulation (39). These unique and inspiring findings indicates that detection of circRNA in body fluids may become a sensitive and specific method in screening and monitoring different cancers. Up to

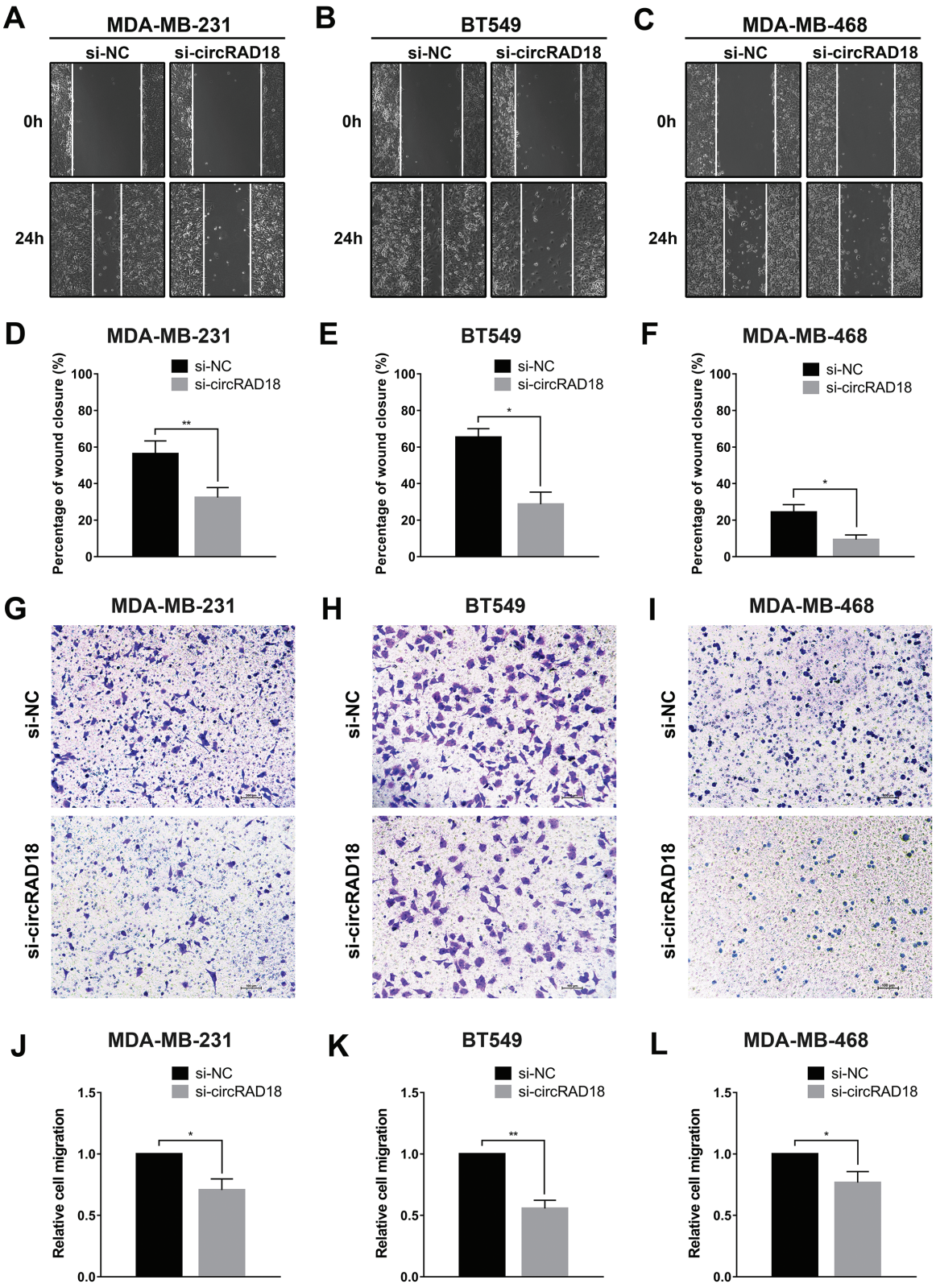

Figure 3. circRAD18 increases metastatic ability of TNBC cell lines. **(A–F)** Knock down of circRAD18 decreases migratory capability of three TNBC cell lines evaluated by wound-healing assays. **(G–L)** Cell migration capacities of three TNBC cell lines were suppressed by silencing circRAD18 detected by transwell assays. *P < 0.05; **P < 0.01.

now, only a few circRNAs have been clearly characterized and functionally studied, whereas the majority of them still remain obscured. In this study, we first identified hsa_circ_0002453 (circRAD18) as a critical circRNA frequently upregulated in TNBC tissues, and high expression of circRAD18 was correlated with TNBC patients' tumor growth and poorer overall survival.

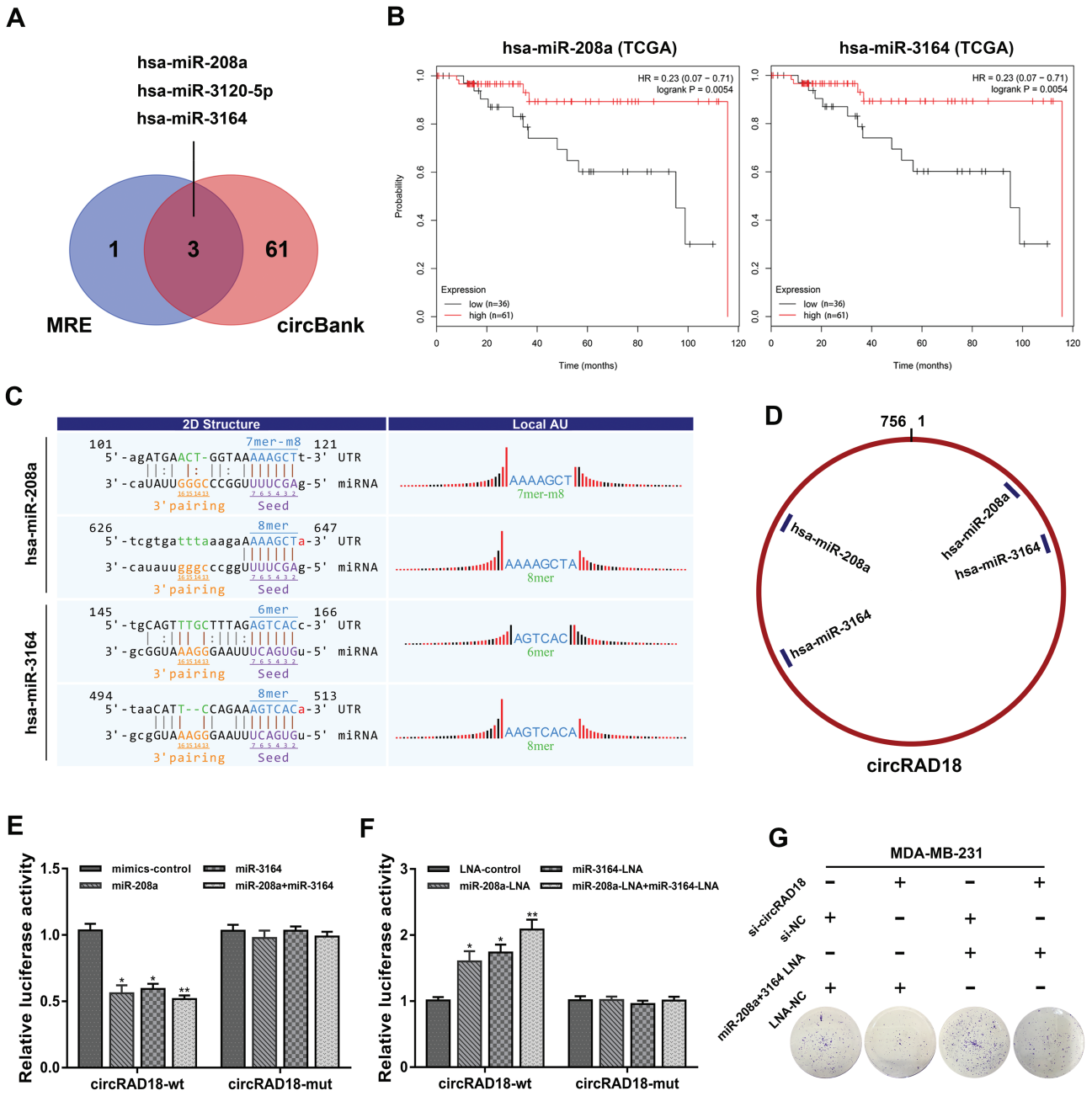

Figure 4. circRAD18 serves as a sponge for miR-208a and miR-3164 in TNBC. **(A)** Potential binding miRNAs of circRAD18 were predicted by MRE and circBank database. **(B)** Kaplan–Meier analysis of the association between miR-208a/3164 and overall survival in TNBC patients from TCGA database. **(C and D)** Schema graph of the predicted binding sites of miR-208a and miR-3164 within the circRAD18. **(E and F)** Relative luciferase activity after co-transfection of a mimic control, miR-208a mimics, miR-3164 mimics, both two mimics, inhibitors-control, miR-208a-inhibitors, miR-3164-inhibitors or both two inhibitors and circRAD18-wt or circRAD18-mut (mutated miRNAs binding sites) luciferase reporter. **(G)** The colony formation ability enhanced by miR-208a and miR-3164 inhibitors were reversed after co-transfected with si-circRAD18 using colony formation assay.

Further mechanistic experiments revealed that circRAD18 sponges miR-208a/3164 to promote TNBC progression through regulating *IGF1/FGF2* expression.

Derived from the *RAD18* gene locus, circRAD18 is composed of exons 3, 4, 5, 6 and 7 and formed by back splicing of the first and last one. Reported by several studies, overexpression of *RAD18* gene enhances cell proliferation, migration and invasion in multiple malignancies (40–43). However, the expression level and precise biological functions of circRAD18 in TNBC was poorly investigated. We validated 31 TNBC and paired adjacent mammary specimens, observing that circRAD18 was overexpressed in over 87% samples. Further verification confirmed the association between its expression level and the clinicopathologic feature (T stage, clinical stage and pathological grade) in 126 TNBC cases. Survival analysis indicated high circRAD18 expression level was an independent predicting factor of poor prognosis for TNBC patients. In loss-off-function experiments, silencing of circRAD18 suppressed cell proliferation, migration and promoted cell apoptosis in three TNBC cell lines. Consistently, knockdown of circRAD18 also inhibited tumor growth in mouse xenograft

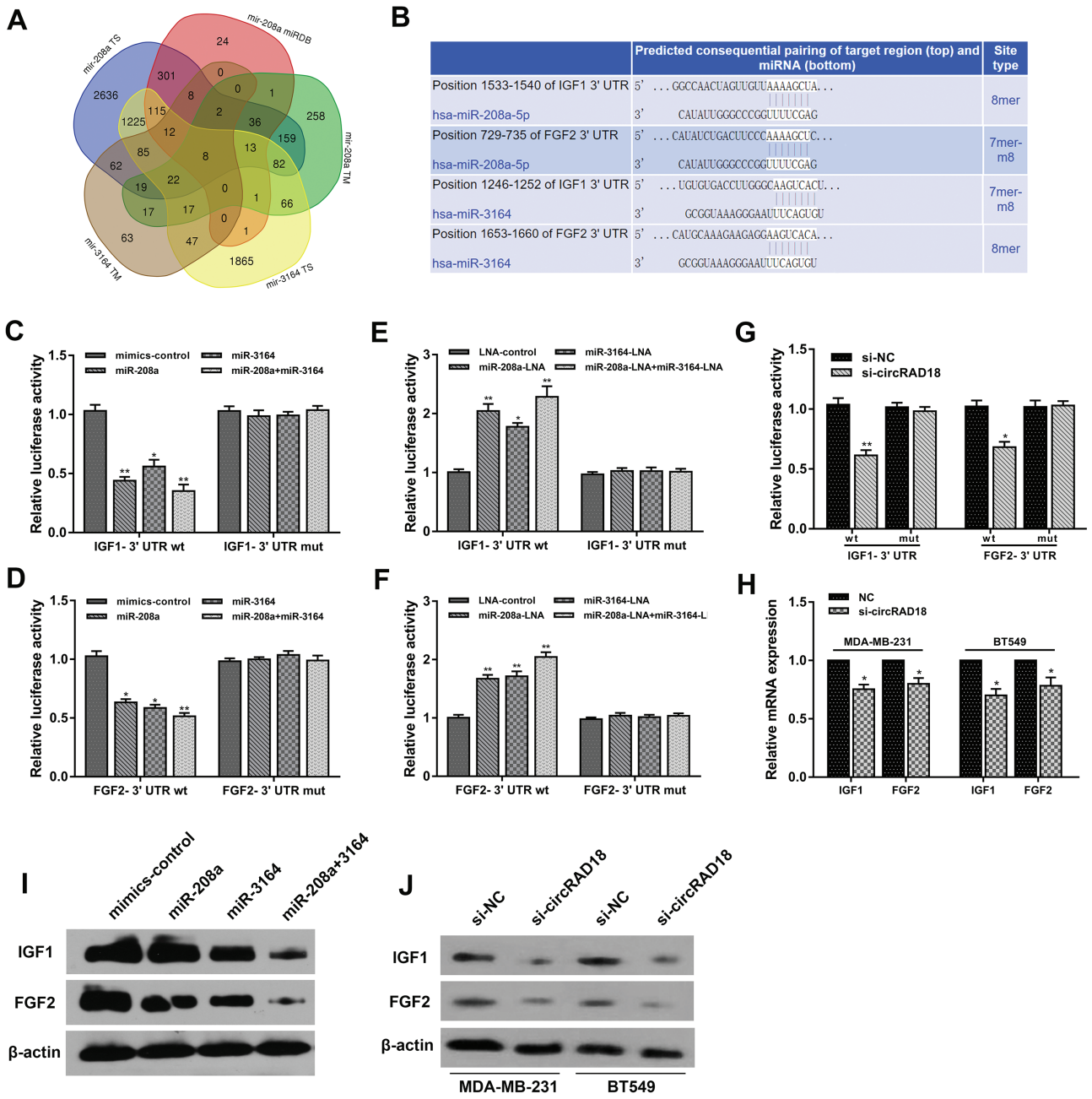

Figure 5. circRAD18 promotes TNBC cell growth and proliferation via circRAD18-miR-208a/3164-*IGF1/FGF2* axis. **(A)** Putative co-targets genes of miR-208a and miR-3164 were predicted based on three algorithms [TargetScan (TS), TargetMiner (TM) and miRDB] depicted by Venn diagram. **(B)** Schema graph of the predicted binding sites of miR-208a and miR-3164 within the 3'-UTR of *IGF1* and *FGF2* mRNA. **(C–F)** Relative luciferase activity after co-transfection of a mimic control, miR-208a mimics, miR-3164 mimics, both two mimics, inhibitors-control, miR-208a-inhibitors, miR-3164-inhibitors or both two inhibitors and *IGF1/FGF2*-3'UTR-wt or *IGF1/FGF2*-3'UTR-mut (mutated miRNAs binding sites) luciferase reporter. **(G)** Luciferase assay of si-circRAD18 effects on *IGF1/FGF2*-3'UTR. **(H)** The impact of knockdown of circRAD18 on *IGF1* and *FGF2* mRNA level in MDA-MB-231 and BT549 cells. **(I)** Both miR-208a/miR-3164 mimics suppressed IGF1 and FGF2 protein expression in MDA-MB-231 cells analyzed by western blot. **(J)** The impact of knockdown of circRAD18 on IGF1 and FGF2 protein expression in MDA-MB-231 and BT549 cells. *P < 0.05; **P < 0.01.

experiment. These results provide insights into the biological significance of circRAD18 and highlight its predictive value for survival in TNBC patients.

On the basis of ceRNA hypothesis, mRNAs, pseudogenes, lncRNAs as well as circRNAs could regulate reciprocally by binding to the MREs. Taking the well-known ciRS-7 as an example, miR-7 was sponged by multiple binding sites of ciRS-7, which might serve as a mediator for complicated biological functions (14). Nevertheless, most of circRNAs lacked convictive experiment to verify the prediction of binding miRNAs. To achieve a better understanding of the molecular mechanism of circRAD18, we utilized MREs analysis and circBank database to predict potential interacting miRNAs. Among the overlap of two predicted results, miR-208a and miR-3164 were both tumor suppressor miRNAs according to TCGA database. Therefore, we presumed them as the targets of circRAD18 and confirmed by dual-luciferase reporter assays. Further 'rescue' experiments manifested that the inhibition of miR-208a or (and) miR-3164 could enhance the colony-forming ability, and this effect could be reversed by circRAD18 knockdown in MDA-MB-231 cells. Subsequently, three algorithms

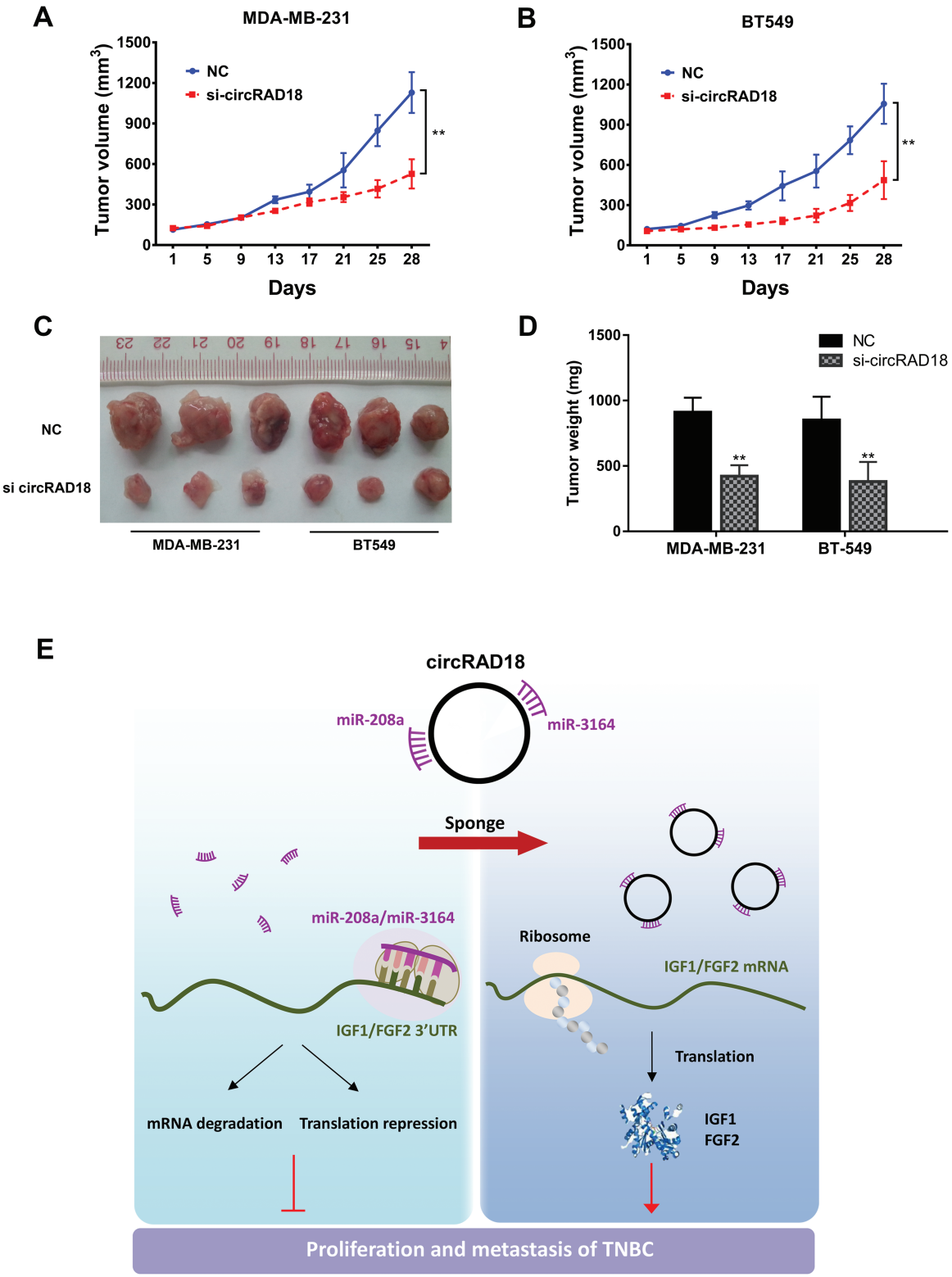

Figure 6. circRAD18 promotes TNBC tumorigenesis *in vivo*. **(A and B)** MDA-MB-231 and BT549 cells were subcutaneously injected into nude mice before continuous intertumoral injection of si-circRAD18 or NC siRNAs. Volume of each tumor was calculated every 4 days and the tumor growth curves are plotted. **(C)** Image of the resected mouse xenograft tumors. **(D)** Tumors from si-circRAD18 or NC treated group were weighted. **(E)** The schematic diagram illustrates the biological mechanism of circRAD18, which serves as a sponge for the miR-208a/3164 to relieve silence for *IGF1* and *FGF2* to promote proliferation and metastasis of TNBC.

(TargetScan, TargetMiner and miRDB) were applied to predict putative co-target oncogenes of miR-208a and miR-3164. Among these candidates, *IGF1* was predicted by all three algorithms, whereas *FGF2* was identified by two. Previous studies have indicated *IGF1* and *FGF2* plays a vital part in the progression of diverse malignancies, including breast cancer, by promoting cancer cell proliferation, invasion and tumor angiogenesis through multiple cell growth signaling (24–31). We demonstrated the regulation of *IGF1*

and *FGF2* by circRAD18 through sponging miR-208a and miR-3164 in TNBC (Figure 6E).

Lacking of effective targeted treatment for TNBC is a rather thorny issue for oncologists; however, decryption of circRAD18 may provide new ideas for TNBC diagnosis or therapy. It can be used as an indicator to predict mortality and recurrence risk for TNBC patients. As an RNA with 756 bases, circRAD18 might be existing in exosomes and secreted into body fluids, which is worthy of studying and proving in the near future. As circRAD18 was overexpressed in non-TNBC breast cancer cell lines, the research on luminal and human epidermal growth factor receptor 2-overexpression subtype breast cancer can also be carried out accordingly.

In summary, our study indicates circRAD18 is upregulated and correlated with more advanced stages and worse clinical outcomes in TNBC. CircRAD18 promotes cell proliferation, migration and inhibites apoptosis through sponging miR-208a/3164 to enhance *IGF1* and *FGF2* expression. Therefore, circRAD18 may serve as a novel prognostic biomarker and potential therapeutic target for TNBC in the future.

Supplementary material

Supplementary data are available at *Carcinogenesis* online.

Funding

This work was supported by funds from the National Natural Science Foundation of China (81772961 to H.T., 81872152 to X.X.)
Conflict of Interest Statement: None declared.

References

1. Bray, F. *et al.* (2018) Global cancer statistics 2018: GLOBOCAN estimates of incidence and mortality worldwide for 36 cancers in 185 countries. CA Cancer J. Clin., 68, 394–424.
2. Siegel, R.L. *et al.* (2019) Cancer statistics, 2019. CA Cancer J. Clin., 69, 7–34.
3. Harbeck, N. *et al.* (2017) Breast cancer. Lancet, 389, 1134–1150.
4. Carey, L. *et al.* (2010) Triple-negative breast cancer: disease entity or title of convenience? Nat. Rev. Clin. Oncol., 7, 683–692.
5. Dent, R. *et al.* (2007) Triple-negative breast cancer: clinical features and patterns of recurrence. Clin. Cancer Res., 13(15 Pt 1), 4429–4434.
6. Xiao, W. *et al.* (2018) Breast cancer subtypes and the risk of distant metastasis at initial diagnosis: a population-based study. Cancer Manag. Res., 10, 5329–5338.
7. Kristensen, L.S. *et al.* (2018) Circular RNAs in cancer: opportunities and challenges in the field. Oncogene, 37, 555–565.
8. Rybak-Wolf, A. *et al.* (2015) Circular RNAs in the mammalian brain are highly abundant, conserved, and dynamically expressed. Mol. Cell, 58, 870–885.
9. Jeck, W.R. *et al.* (2013) Circular RNAs are abundant, conserved, and associated with ALU repeats. RNA, 19, 141–157.
10. Conn, S.J. *et al.* (2015) The RNA binding protein quaking regulates formation of circRNAs. Cell, 160, 1125–1134.
11. Zhang, X.O. *et al.* (2014) Complementary sequence-mediated exon circularization. Cell, 159, 134–147.
12. Li, X. *et al.* (2018) The biogenesis, functions, and challenges of circular RNAs. Mol. Cell, 71, 428–442.
13. Salmena, L. *et al.* (2011) A ceRNA hypothesis: the Rosetta stone of a hidden RNA language? Cell, 146, 353–358.
14. Hansen, T.B. *et al.* (2013) Natural RNA circles function as efficient microRNA sponges. Nature, 495, 384–388.
15. Pan, H. *et al.* (2018) Overexpression of Circular RNA ciRS-7 Abrogates the tumor suppressive effect of miR-7 on gastric cancer via PTEN/PI3K/AKT signaling pathway. J. Cell. Biochem., 119, 440–446.
16. Su, C. *et al.* (2018) CiRS-7 targeting miR-7 modulates the progression of non-small cell lung cancer in a manner dependent on NF-κB signalling. J. Cell. Mol. Med., 22, 3097–3107.
17. Li, R.C. *et al.* (2018) CiRS-7 promotes growth and metastasis of esophageal squamous cell carcinoma via regulation of miR-7/HOXB13. Cell Death Dis., 9, 838.
18. Weng, W. *et al.* (2017) Circular RNA ciRS-7-A promising prognostic biomarker and a potential therapeutic target in colorectal cancer. Clin. Cancer Res., 23, 3918–3928.
19. Zheng, Q. *et al.* (2016) Circular RNA profiling reveals an abundant circHIPK3 that regulates cell growth by sponging multiple miRNAs. Nat. Commun., 7, 11215.
20. Chen, B. *et al.* (2018) circEPSTI1 as a prognostic marker and mediator of triple-negative breast cancer progression. Theranostics, 8, 4003–4015.
21. Agarwal, V. *et al.* (2015). Predicting effective microRNA target sites in mammalian mRNAs. Elife, 4. doi:10.7554/eLife.05005
22. Bandyopadhyay, S. *et al.* (2009) TargetMiner: microRNA target prediction with systematic identification of tissue-specific negative examples. Bioinformatics, 25, 2625–2631.
23. Wong, N. *et al.* (2015) miRDB: an online resource for microRNA target prediction and functional annotations. Nucleic Acids Res., 43, D146–D152.
24. Suyama, K. *et al.* (2002) A signaling pathway leading to metastasis is controlled by N-cadherin and the FGF receptor. Cancer Cell, 2, 301–314.
25. Chandler, L.A. *et al.* (1999) Prevalent expression of fibroblast growth factor (FGF) receptors and FGF2 in human tumor cell lines. Int. J. Cancer, 81, 451–458.
26. LeRoith, D. *et al.* (2003) The insulin-like growth factor system and cancer. Cancer Lett., 195, 127–137.
27. Belfiore, A. *et al.* (2008) IGF and insulin receptor signaling in breast cancer. J. Mammary Gland Biol. Neoplasia, 13, 381–406.
28. De Francesco, E.M. *et al.* (2017) GPER mediates the angiocrine actions induced by IGF1 through the HIF-1α/VEGF pathway in the breast tumor microenvironment. Breast Cancer Res., 19, 129.
29. Eswarakumar, V.P. *et al.* (2005) Cellular signaling by fibroblast growth factor receptors. Cytokine Growth Factor Rev, 16, 139–149.
30. Schelch, K. *et al.* (2018) FGF2 and EGF induce epithelial-mesenchymal transition in malignant pleural mesothelioma cells via a MAPKinase/MMP1 signal. Carcinogenesis, 39, 534–545.
31. Pacher, M. *et al.* (2007) Impact of constitutive IGF1/IGF2 stimulation on the transcriptional program of human breast cancer cells. Carcinogenesis, 28, 49–59.
32. Memczak, S. *et al.* (2013) Circular RNAs are a large class of animal RNAs with regulatory potency. Nature, 495, 333–338.
33. Qiu, M. *et al.* (2018) The circular RNA circPRKCI promotes tumor growth in lung adenocarcinoma. Cancer Res., 78, 2839–2851.
34. Zhan, W. *et al.* (2018). circCTIC1 promotes the self-renewal of colon TICs through BPTF-dependent c-Myc expression. Carcinogenesis., 40, 560–568.
35. He, R. *et al.* (2017) circGFRA1 and GFRA1 act as ceRNAs in triple negative breast cancer by regulating miR-34a. J. Exp. Clin. Cancer Res., 36, 145.
36. Zhang, J. *et al.* (2017) Circular RNA_LARP4 inhibits cell proliferation and invasion of gastric cancer by sponging miR-424-5p and regulating LATS1 expression. Mol. Cancer, 16, 151.
37. Yao, Z. *et al.* (2017) ZKSCAN1 gene and its related circular RNA (circZKSCAN1) both inhibit hepatocellular carcinoma cell growth, migration, and invasion but through different signaling pathways. Mol. Oncol., 11, 422–437.
38. Chen, X. *et al.* (2018) PRMT5 Circular RNA promotes metastasis of urothelial carcinoma of the bladder through sponging miR-30c to induce epithelial-mesenchymal transition. Clin. Cancer Res., 24, 6319–6330.
39. Li, Z. *et al.* (2018) Tumor-released exosomal circular RNA PDE8A promotes invasive growth via the miR-338/MACC1/MET pathway in pancreatic cancer. Cancer Lett., 432, 237–250.
40. Zou, S. *et al.* (2018) RAD18 promotes the migration and invasion of esophageal squamous cell cancer via the JNK-MMPs pathway. Cancer Lett., 417, 65–74.
41. Wong, R.P. *et al.* (2012) Elevated expression of Rad18 regulates melanoma cell proliferation. Pigment Cell Melanoma Res., 25, 213–218.
42. Yang, Y. *et al.* (2018) Diverse roles of RAD18 and Y-family DNA polymerases in tumorigenesis. Cell Cycle, 17, 833–843.
43. Tanoue, Y. *et al.* (2018) Differential roles of Rad18 and Chk2 in genome maintenance and skin carcinogenesis following UV exposure. J. Invest. Dermatol., 138, 2550–2557.